Preparation of High Adsorption Performance and Stable Biochar Granules by $FeCl_3$-Catalyzed Fast Pyrolysis

De-Chang Li,[a] Jin-Wen Ding,[b] Ting-Ting Qian,[a] Shun Zhang[a] and Hong Jiang[a*]

[a.] CAS Key Laboratory of Urban Pollutant Conversion, Department of Chemistry, University of Science and Technology of China, Hefei 230026, China

[b.] CAS Key Laboratory of Materials for Energy Conversion, Department of Materials Science and Engineering, University of Science and Technology of China, Hefei 230026, China

* Corresponding author: Dr. Hong Jiang

E-mail: jhong@ustc.edu.cn

R_{ss} determination. To confirm the accuracy of scatter ratio (SR), concentrations of suspended substance (R_{SS}) under the same conditions as the SR determination experiment were determined and calculated according to the following equation.

$$R_{ss} = \frac{M_{ss}}{V}$$

As shown in the Table S6, the mass distributed in solution (M_{ss}) is approximate to that of the decreased mass of GBC (M_0-M), which means that both SR and R_{ss} are suitable indexes for the stability of GBCs. Considering the GBC remainder is easier to separate for determination, we decided to employ scatter ratio (SR) to examine the physical stability of GBC.

XPS analysis. The main functional groups and relative peak area percentages of C and O are listed in Table S2. The main functional groups containing O are C–O (533.0 eV) and silicon-oxygen bond (531.8 eV, 532.4 eV) for both GBCs. The peak at 531.2 eV which can be assigned to Al_2O_3 or FeOOH gets stronger after $FeCl_3$ doping.[S1]

Table S1. Components of the kaolin used in this work.

Component	SiO_2	Al_2O_3	K_2O	Na_2O	Fe_2O_3	MgO	CaO	TiO_2
Content (%,wt)	47.73	43.36	3.75	2.04	1.24	0.89	0.15	0.31

Table S2. Physical characteristics of Fe_0-GBC_{650} and Fe_5-GBC_{650}.

Sample	**BET surface area m^2/g**	**Pore volume cm^3/g**	**Average pore width Å**
Fe_0-GBC_{650}	38.46	0.0302	31.40
Fe_5-GBC_{650}	78.62	0.0543	27.65

Table S3. Curve fitting results of XPS C 1s and O 1s spectra of GBCs.

Elements	**Fe_0-GBC_{650}**			**Fe_5-GBC_{650}**		
	Groups	B. E. (eV)	Area percentage (%)	Groups	B. E. (eV)	Area percentage (%)
C 1s	C=C	284.3	15.45	C=C	284.3	21.01
	Graphite C	284.8	31.11	Graphite C	284.8	15.67
	C–C	285.2	32.33	C–C	285.3	32.79
	C–O	286.7	21.11	C–O	286.7	30.52
O 1s	Al_2O_3	531.2	10.64	Al_2O_3/FeOOH	531.2	18.53
	SiO_3^{2-}	531.8	19.86	SiO_3^{2-}	531.9	23.44
	SiO_2	532.4	26.11	SiO_2	532.4	24.47
	C–O	533.0	26.11	C–O	533.0	21.54
	O–C=O	533.6	17.28	O–C=O	533.6	12.02

Table S4. Summary of 4-CP adsorption capacities of various adsorbents.

Adsorbent	4-CP adsorption capacity (mg/g)	Reference
Activated carbon	412	S2
Biosolid biochar	~45	S3
Granular activated carbon	200	S3
Rice straw biochar	~10	S3
Fallen leaves biochar	~10	S3
Rice straw biochar	~25	S4
Granular activated carbon	~80	S5
Activated carbon	188.7	S6
Biochar in Fe_5-GBC_{650}	250.0	**This work**

Table S5. Biochar production rates of GBCs prepared with different $FeCl_3$ dosages.

Sample	Yield (%)
Fe_0-GBC_{650}	20.6
Fe_1-GBC_{650}	30.4
Fe_3-GBC_{650}	48.9
Fe_5-GBC_{650}	52.2

Table S6. Related data on R_{SS} and SR determination.

	M_0 (mg)	M (mg)	M_{SS} (mg)	M_0-M (mg)	R_{SS} (mg/L)	SR (%)
Fe_0-GBC_{650}	270.3	138.5	129.3	131.8	4310.0	48.8
	267.4	154.1	111.7	113.3	3723.3	42.4
	270.2	142.0	128.6	128.2	4286.7	47.4
Fe_5-GBC_{650}	306.7	302.4	6.3	4.3	210	1.4
	311.2	299.9	13.0	11.3	433.3	3.6
	310.6	303.1	8.6	7.5	286.7	2.4

Table S7. Scatter ratios of GBCs in different pH aqueous systems.

Sample	pH	SR (%)	Sample	pH	SR (%)
Fe_0-GBC_{650}	5.0	45.61	Fe_5-GBC_{650}	5.0	2.76
Fe_0-GBC_{650}	6.0	45.96	Fe_5-GBC_{650}	6.0	2.86
Fe_0-GBC_{650}	7.0	44.97	Fe_5-GBC_{650}	7.0	2.50
Fe_0-GBC_{650}	8.0	45.01	Fe_5-GBC_{650}	8.0	2.34
Fe_0-GBC_{650}	9.0	45.20	Fe_5-GBC_{650}	9.0	2.93

Table S8. Compressive strengths of different kind of GBCs.

Sample	Average maximum compressive load (N)	Average maximum compressive stress (MPa)
Fe_0-GBC_{500}	12.29	1.12
Fe_5-GBC_{650}	49.97	4.86
NaCl-GBC_{650}	9.43	0.79
$Fe(NO_3)_3$-GBC_{650}	4.72	0.43
NaCl-$Fe(NO_3)_3$-GBC_{650}	28.56	2.51

References

S1 X. Zhu, Y. Liu, C. Zhou, S. Zhang and J. Chen, *ACS Sustain. Chem. Eng.*, 2014, **2**, 969-977.

S2 V. M. Monsalvo, A. F. Mohedano and J. J. Rodriguez, *Desalination*, 2011, **277**, 377-382.

S3 S.-Y. Oh and Y.-D. Seo, *Environ. Sci. Pollut. Res.*, 2015, 1-11.

S4 Y.-h. Shih, Y.-f. Su, R.-y. Ho, P.-h. Su and C.-y. Yang, *Sci. Total. Environ.*, 2012, **433**, 523-529.

S5 O. Hamdaoui and E. Naffrechoux, *Ultrason. Sonochem.*, 2009, **16**, 15-22.

S6 B. H. Hameed, L. H. Chin and S. Rengaraj, *Desalination*, 2008, **225**, 185-198.

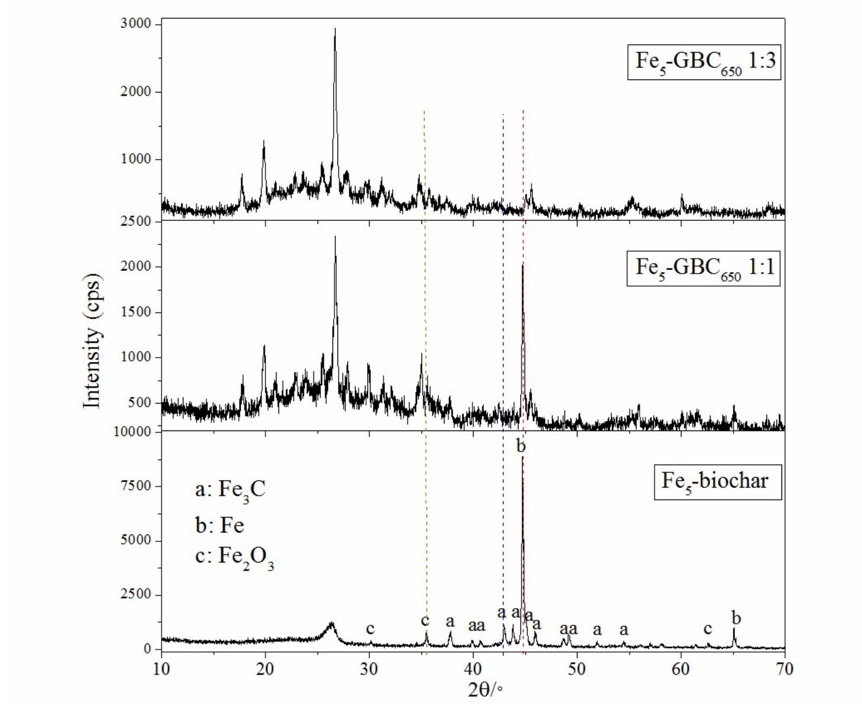

Figure S1. XRD results of GBCs with different mass ratios between kaolin and sawdust.

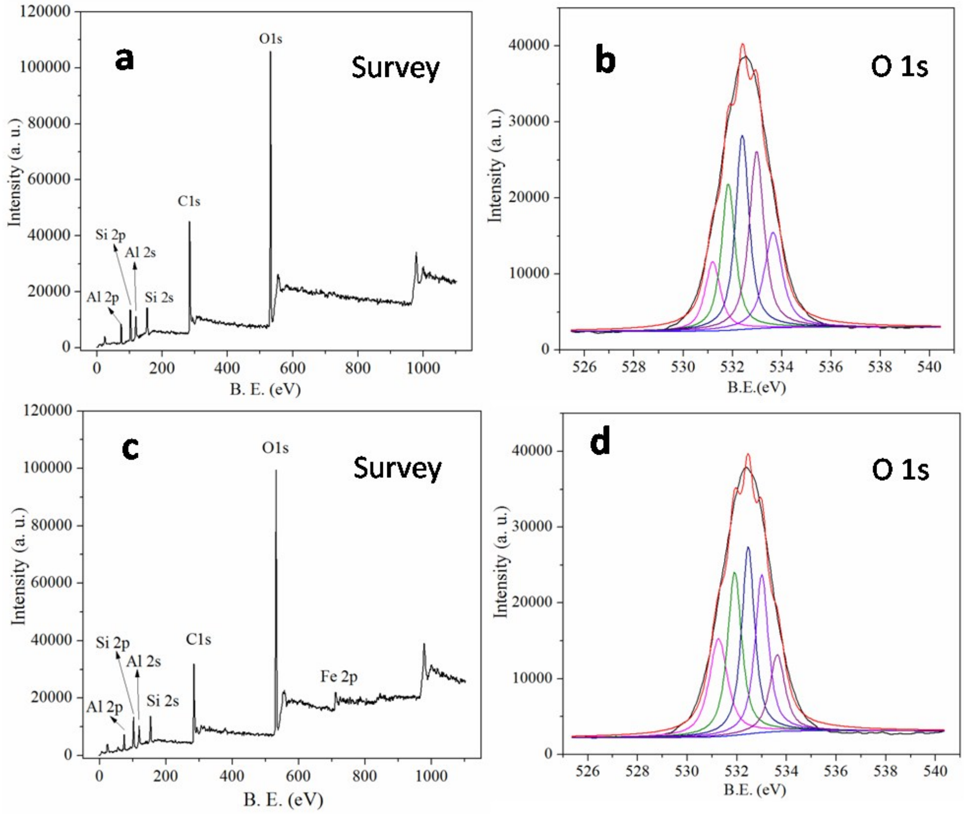

Figure S2. a,b) XPS results of Fe_0-GBC_{650}; c,d) XPS results of Fe_5-GBC_{650}.

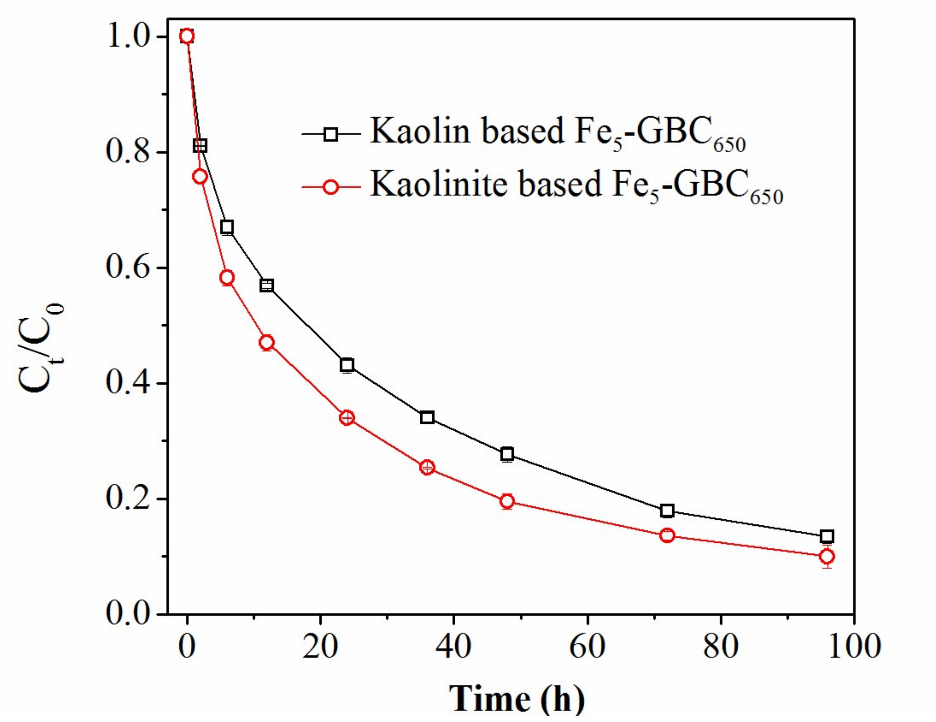

Figure S3. Comparison of kaolin-based and kaolinite-based Fe_5-GBC_{650} on 4-CP adsorption.

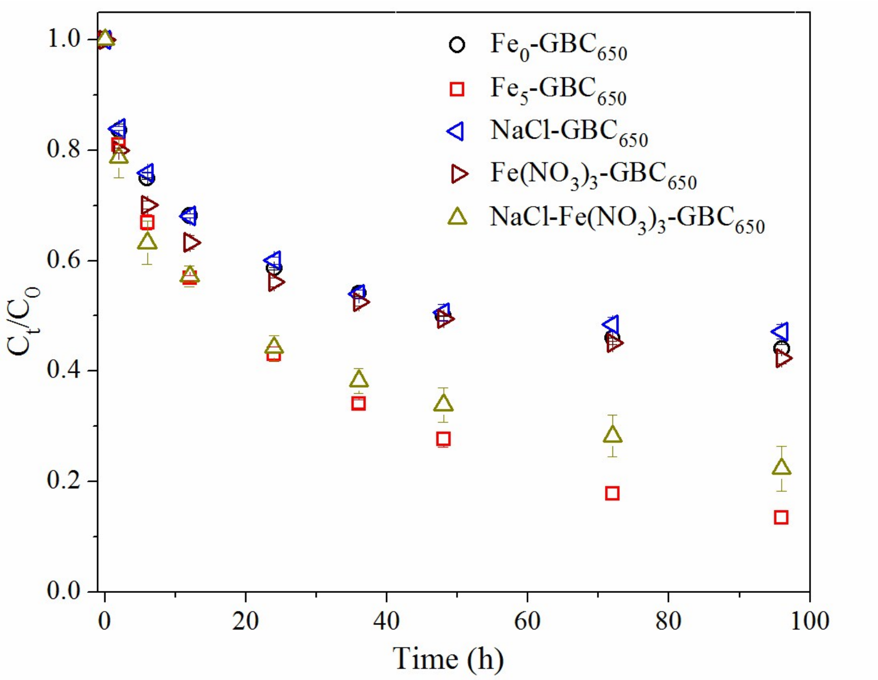

Figure S4. Performance of different adsorbents on 4-CP adsorption

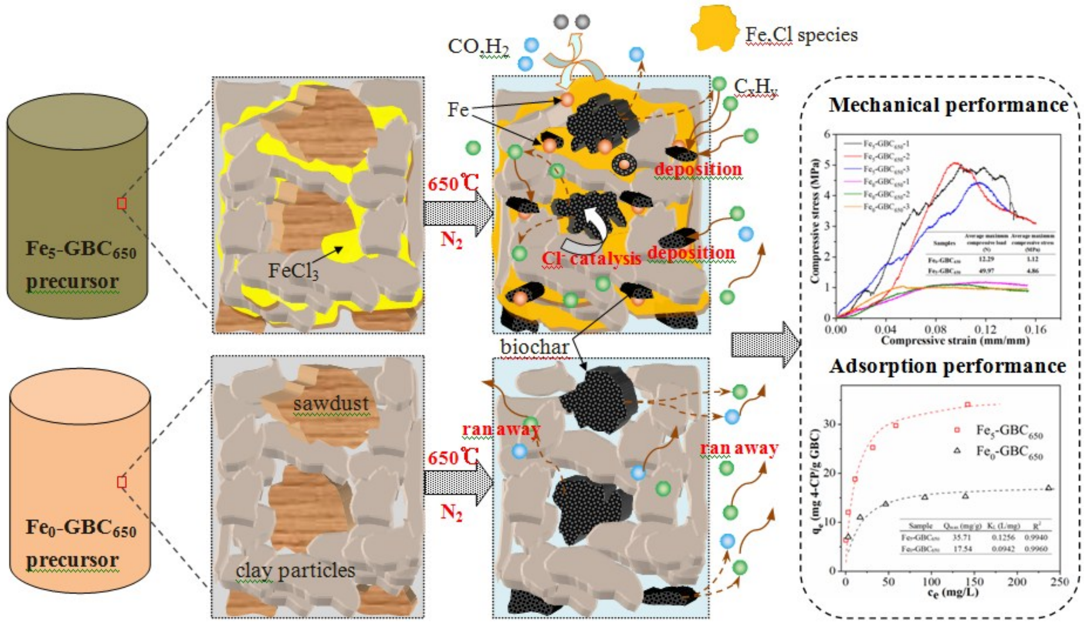

Figure S5. Schematic for work mechanism of $FeCl_3$ to enhance the sorption of 4-CP and mechanical performance.